tvst

https://doi.org/10.1167/tvst.8.3.15

Article

Repeatability of Fluorescence Lifetime Imaging Ophthalmoscopy in Normal Subjects With Mydriasis

Soonil Kwon[1,2], Enrico Borrelli[1], Wenying Fan[1], Adel Ebraheem[1], Kenneth M. Marion[1], and SriniVas R. Sadda[1,3]

[1] Doheny Eye Institute, Los Angeles, CA, USA
[2] Department of Ophthalmology, Hallym Sacred Heart Hospital, Hallym University College of Medicine, Anyang, Gyeonggi, South Korea
[3] Department of Ophthalmology, David Geffen School of Medicine at UCLA, Stein Eye Institute, Los Angeles CA, USA

Correspondence: SriniVas R. Sadda, MD, Doheny Eye Institute, PO Box 86228, Los Angeles, CA 90086, USA. e-mail: ssadda@doheny.org

Received: 21 November 2018
Accepted: 10 February 2019
Published: 8 May 2019

Keywords: repeatability; fluorescence lifetime; Fluorescence Lifetime Imaging Ophthalmoscopy

Citation: Kwon S, Borrelli E, Fan W, Ebraheem A, Marion KM, Sadda SR. Repeatability of Fluorescence Lifetime Imaging Ophthalmoscopy in normal subjects with mydriasis. Trans Vis Sci Tech. 2019;8(3):15, https://doi.org/10.1167/tvst.8.3.15

Purpose: We evaluate the repeatability of fluorescence lifetime imaging ophthalmoscopy (FLIO) in normal subjects with mydriasis and explore factors that influence FLIO imaging.

Method: Thirty-two healthy participants (63 eyes) were enrolled in this prospective study. The Heidelberg Engineering FLIO system uses a 473 nm blue laser light and the emitted fluorescence is detected in two wavelength channels, short and long spectral channels (SSC, LSC). The mean fluorescence lifetime (τ_m) values were computed for the entire scan area as well as in five regions of interest (ROI, 1 × 1 mm) at the fovea and superior, nasal, inferior, and temporal portions of the macula. Intraclass correlation coefficients (ICC) and coefficients of variation (CV) were used to assess the repeatability. Age, macular thickness, and vascular density also were correlated with τ_m.

Results: The repeatability was good for both channels (ICC, 0.956∼0.995; CV, 9∼16%). The τ_m for the entire scan was 367.8 ± 58.1 picoseconds (ps) in SSC and 322.5 ± 34.0 ps in LSC. τ_m was the shortest in the fovea and significantly shorter in the temporal region compared to other regions. τ_m was positively correlated with age ($r = 0.588$ for SSC and $r = 0.584$ for LSC, $P = 0.000$) and retinal thickness ($r = 0.298$ for SSC and $r = 0.322$ for LSC, $P = 0.000$), and negatively correlated with vascular density ($r = -0.112$, $P = 0.055$ for SSC and $r = -0.119$, $P = 0.040$ for LSC).

Conclusion: Repeatable fluorescence lifetime values can be obtained with FLIO, but the lifetimes are affected by age, retinal thickness, vessel density, and macular location.

Translational Relevance: Establishing repeatability of FLIO can introduce fluorescence lifetime imaging technique, which is used in basic science for analysis of excitation and emission wavelength spectrum of fixed and living cells into clinical practice.

Introduction

The retina possesses a wide range of endogenous fluorophores, including lipofuscin, advanced glycation end products (AGE), collagen, and elastin.[1–3] The detection and discrimination of these fluorophores may be of value in elucidating metabolic and functional alterations in the context of various retinal diseases. In principle, these fluorophores can be discriminated by measuring specific excitation and emission spectra. However, any discrimination of fundus fluorophores by specific excitation and emission spectra is limited by the efficiency of transmission through the ocular media, allowing spectral investigations in the wavelength range between 400 and 900 nm. Fluorescence lifetime imaging ophthalmoscopy (FLIO) is a relatively novel technique that allows fluorophores to be detected and potentially discriminated using their fluorescence lifetime.[1,4] With the FLIO technique, the autofluorescence

molecules of the retina are excited with laser pulses and the measured time duration between laser pulse and the detection of the fluorescent photon represents the time the excited fluorophore spends in its higher energy level before returning to its ground state by releasing typically a longer-wavelength photon. Because each fluorophore possesses a characteristic fluorescence lifetime, which also is influenced by its environment, the histogram of photon arrival times representing the decay of fluorescence intensity after several excitation cycles permits the differentiation of fluorophores with overlapping emission spectra. A quantitative image can be generated based on the lifetimes of the different endogenous retinal fluorophores.[5,6] Thus, fluorescence lifetime measurements provide additional information and contrast compared to conventional fluorescence imaging based on intensity alone. It has been reported that FLIO in the human retina has the potential to reveal functional changes related to various eye and systemic diseases, such as early stages of diabetic retinopathy, Alzheimer's disease, Stargardt disease, age-related macular degeneration, and other pathologies.[6–9]

In a previous report assessing healthy retina, mean fluorescence lifetimes were shortest in the central fovea and longest in the area of the optic disc and vessels.[5] Age and retinal thickness also influenced fluorescence lifetime.[5] Although the longest lifetimes were found in the regions of large retinal blood vessels, the impact of smaller vessels and capillaries on lifetimes was not explored. In addition, in a previous study we observed that nondilated pupils might yield longer lifetimes, and suggested that mydriasis and maintenance of a consistent and stable pupil might yield more reliable results.[10]

The discriminative power of any diagnostic technique, however, is only as meaningful as the reliability and repeatability of the assay. Thus, we evaluated the repeatability of FLIO in the posterior pole of normal subjects with mydriasis and explored the factors that could influence the fluorescence lifetime values, including macular region, retinal thickness, and retinal vessel density.

Methods

Subjects

In this prospective, observational, single-center study at the Doheny UCLA Eye Centers, we recruited 32 healthy, phakic volunteers aged 20 to 70 years. Subjects had no history of medical or ophthalmic disease, as confirmed by chart review and ophthalmic exam. Written informed consent was obtained from all individuals before study participation. The study was approved by the institutional review board of the University of California, Los Angeles. The study complied with the requirements of the Health Insurance Portability and Accessibility Act and adhered to the tenets of the Declaration of Helsinki. Written, informed consent was obtained from all subjects before imaging.

Study Design

All subjects underwent detailed clinical examination, including autorefraction using ARK-530 (Nidek Co. Ltd., Gamagori, Japan), best corrected visual acuity (BCVA), intraocular pressure measurement, slit-lamp biomicroscopy, ultrawide-field fundus photo using an Optos 200Tx (Optos, Dunfermline, UK), and optical coherence tomography using a Cirrus HD-OCT model 5000 with Angioplex (Carl Zeiss Meditec, Dublin, CA). FLIO testing was performed in both eyes following dilation using a prototype Heidelberg FLIO device (Heidelberg, Germany) which is described in further detail below. Two FLIO acquisitions were performed in a dark room during the course of the day with an interval between tests of at least 1 hour. The pupil was dilated to at least 7 mm in diameter using tropicamide 0.5% and phenylephrine HCl 2.5%. All FLIO measurements were acquired by one operator (S.K.).

Setting for FLIO

Basic principles of the FLIO technique have been describe in previous reports.[5,6,11] In short, the prototype FLIO device used a pulsed blue laser with an excitation wavelength of 473 nm with 80 MHz repetition rate, as the excitation source for retinal fluorescence. The fluorescent light was detected by highly sensitive hybrid detectors in two different spectral ranges (short spectral channel [SSC]; wavelength 498 to 560 nm), long spectral channel [LSC]; wavelength 560–720 nm) and registered by time-correlated single photon counting (TCSPC) cards. Autofluorescence images were detected simultaneously with a confocal high-contrast infrared image, which was used for adjusting spatial location by the system to record each photon to the corresponding image pixel. The macula was centrally adjusted in the FLIO exam, and the number of collected photons was at least 1000 photons per pixel for every retinal location to insure an adequate signal-to-noise ratio.

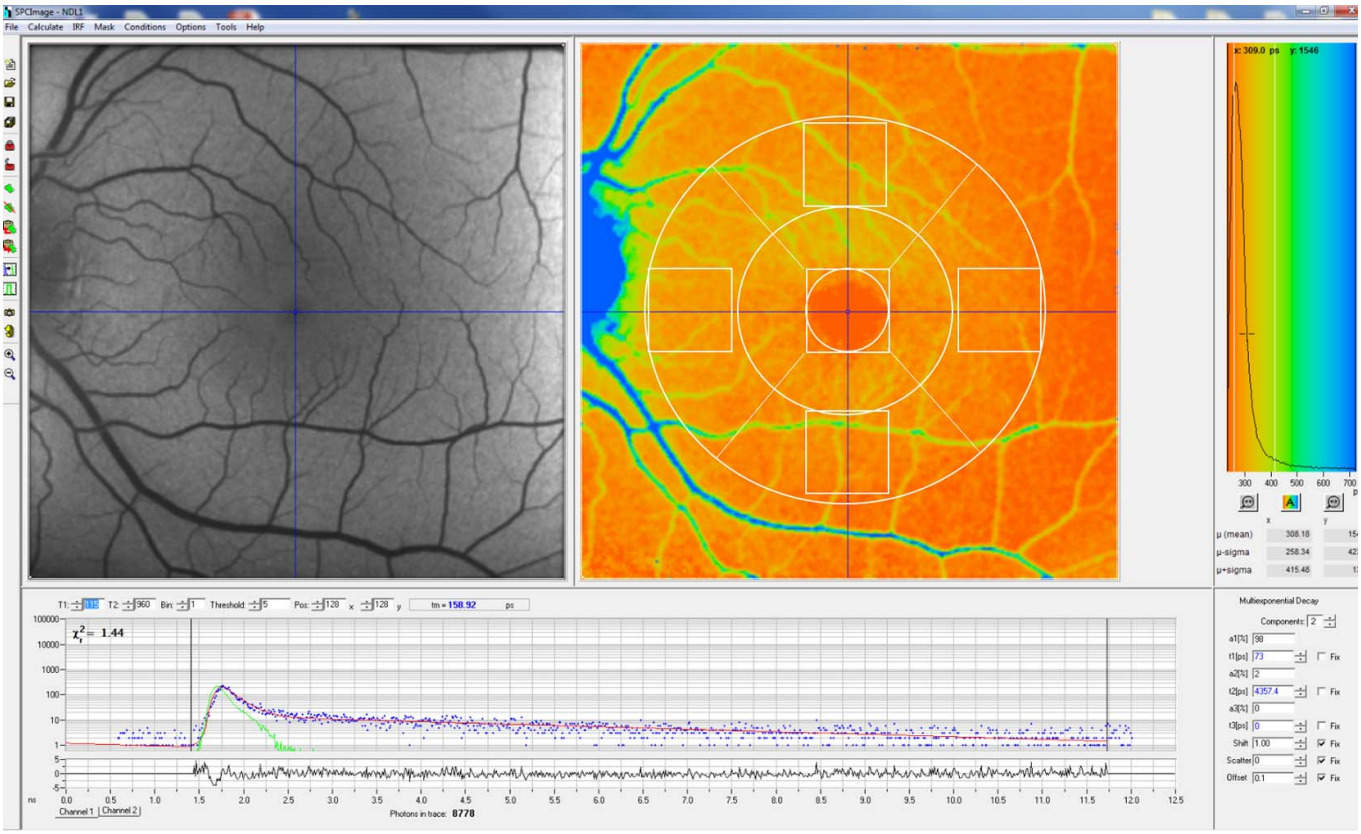

Figure 1. Autofluorescence image (*left*) and companion fluorescence lifetime map (*right*) with overlaid ETDRS grid illustrating the location of the five ROIs (each a 1 × 1 mm square; 28 × 28 pixel).

Data Analysis

The software SPCImage 4.4.2 (Becker & Hickl GmbH, Berlin, Germany) was used for the fluorescence decay analysis. A 3 × 3 pixel binning was used in both channels, the resultant data were fitted triexponentially. Thus, the fluorescence decay function was effectively allocated to three components, and thereby described through the lifetime parameters $\tau_{1\sim3}$ and amplitudes $a_{1\sim3}$. For a global characterization of the fluorescence, an amplitude-weighted mean fluorescence lifetime value τ_m for each pixel was calculated as follows:

$$\tau_m = \frac{a1 * \tau1 + a2 * \tau2 + a1 * \tau3}{a1 + a2 + a3}$$

The "goodness" of the exponential fit of the exponential decay function was indicated by the χ^2 value. To assess whether the repeatability of the fluorescence lifetime values were affected by the fundus region, lifetime values were computed from five macular regions (each region consisting of a square 28 × 28 pixels in size): fovea, superior, inferior, nasal, and temporal macula (Fig. 1).

Structural macular cube 512 × 128 scans covering a 6 × 6 mm macular area centered on the fovea and optical coherence tomography angiography (OCTA) imaging of the macula covering a 6 × 6 mm area centered on the fovea using Food and Drug Administration (FDA)–cleared OCTA software (Cirrus Angioplex software version 6.0) were obtained using the Cirrus 5000 with Angioplex. Retinal thickness values in the regions corresponding to the lifetime measurements were computed using the instrument software. OCTA was obtained to assess whether the small vessel circulation and density of these vessels could have any impact on lifetimes. A semiautomated algorithm was used to quantify vessel density (VD) on the OCTA images. Briefly, the two-dimensional (2D) en face 6 × 6 mm fovea-centered OCTA image of whole retina was first converted to an 8-bit image (524 × 524 pixels). Then, using Image J, the image was converted into a binary image by a three-step method. First, the image was processed

Table 1. Demographics of the Subjects

Number of subjects (eyes)	32 (63)
Age	36.3 ± 10.7
Sex, M:F)	17:15
Lens status, eyes, phakic:pseudophakic	63:0
Spherical equivalent, mean ± SD, D	
Right eye	−1.8 ± 2.6
Left eye	−1.9 ± 2.6

using a top-hat filter with a window size of 12 pixels to remove uneven illumination. Global and local thresholding (median method) was used separately to create two binary images. Finally, two binary images were combined to create the final binarized version by including the pixels detected by both binary methods. A similar approach has been reported previously.[12,13]

Statistical Analysis

Statistical analysis of the data was performed using SPSS 23.0 software (IBM Corporation, Armonk, NY). For the test–retest reliability, the τ_m of the entire macula and the five prespecified regions were compared between the first and second tests using intraclass correlation coefficients (ICC) and Bland-Altman plots. The differences among the five regions were investigated by Student's *t*-test and the variability of fluorescence lifetime values was assessed by interindividual coefficients of variation (CV). Pearson's correlation and simple linear regression models were constructed to evaluate for factors that could influence the fluorescence lifetime, such as age, refractive error, retinal thickness, and vascular density. Generalized estimating equations (GEE) were used to account for correlations between eyes. Statistical results were expressed as *P* values and a $P < 0.05$ was considered statistically significant.

Results

One volunteer declined to have both eyes dilated due to personal reasons, and thus a total of 63 eyes from 32 healthy subjects (mean age, 36.3 ± 10.7 years; range, 25–67; 47% female subjects) were included in this study. Mean spherical equivalent was −1.8 ± 2.6 diopters (D) in right eye and −1.9 ± 2.6 D in left eye (Table 1).

Repeatability and Topographic Distribution of Lifetime

The repeatability of fluorescence lifetime between two sessions was evaluated for the entire macula as well as the five prespecified regions in both spectral channels (SSC and LSC). The repeatability of the τ_m for each group is shown in Table 2. A high level of repeatability for τ_m (ICC, 0.956∼0.995) was observed for both channels of both eyes. Figure 2 shows the combined Bland-Altman plots for the agreement of τ_m between two measurements in all regions for both spectral channels.

The τ_m measured in the entire macula was 367.8 ± 58.1 picoseconds (ps) in the SSC and 322.5 ± 34.0 ps in the LSC. The foveal region featured the shortest τ_m among the five predefined regions in both spectral channels (248.9 ± 40.8 ps in SSC, 255.4 ± 28.9 ps in LSC). The temporal area showed significantly shorter lifetime compared to other regions in both spectral channels (Table 3, Fig. 3). The lifetime of the superior region in the LSC was significantly shorter than the inferior and nasal area, but not significant in SSC (Fig. 3).

The CVs in the SSC were 11%∼16% and 9%∼11% in LSC. The CV was slightly higher in the foveal area

Table 2. The Repeatability of Mean Fluorescence Lifetime (τ_m)

	Channel, ICC (95% CI)			
Area	Rt. SSC	Rt. LSC	Lt. SSC	Lt. LSC
Total	0.977 (0.952–0.989)	0.987 (0.973–0.994)	0.976 (0.952–0.989)	0.988 (0.974–0.994)
Fovea	0.956 (0.908–0.979)	0.979 (0.955–0.990)	0.977 (0.953–0.989)	0.993 (0.985–0.996)
Superior	0.971 (0.941–0.986)	0.989 (0.977–0.995)	0.979 (0.958–0.990)	0.995 (0.990–0.998)
Inferior	0.959 (0.914–0.980)	0.985 (0.969–0.993)	0.978 (0.954–0.989)	0.993 (0.985–0.997)
Nasal	0.971 (0.939–0.986)	0.986 (0.971–0.993)	0.982 (0.963–0.991)	0.991 (0.982–0.996)
Temporal	0.961 (0.919–0.981)	0.987 (0.974–0.994)	0.985 (0.969–0.993)	0.994 (0.988–0.997)

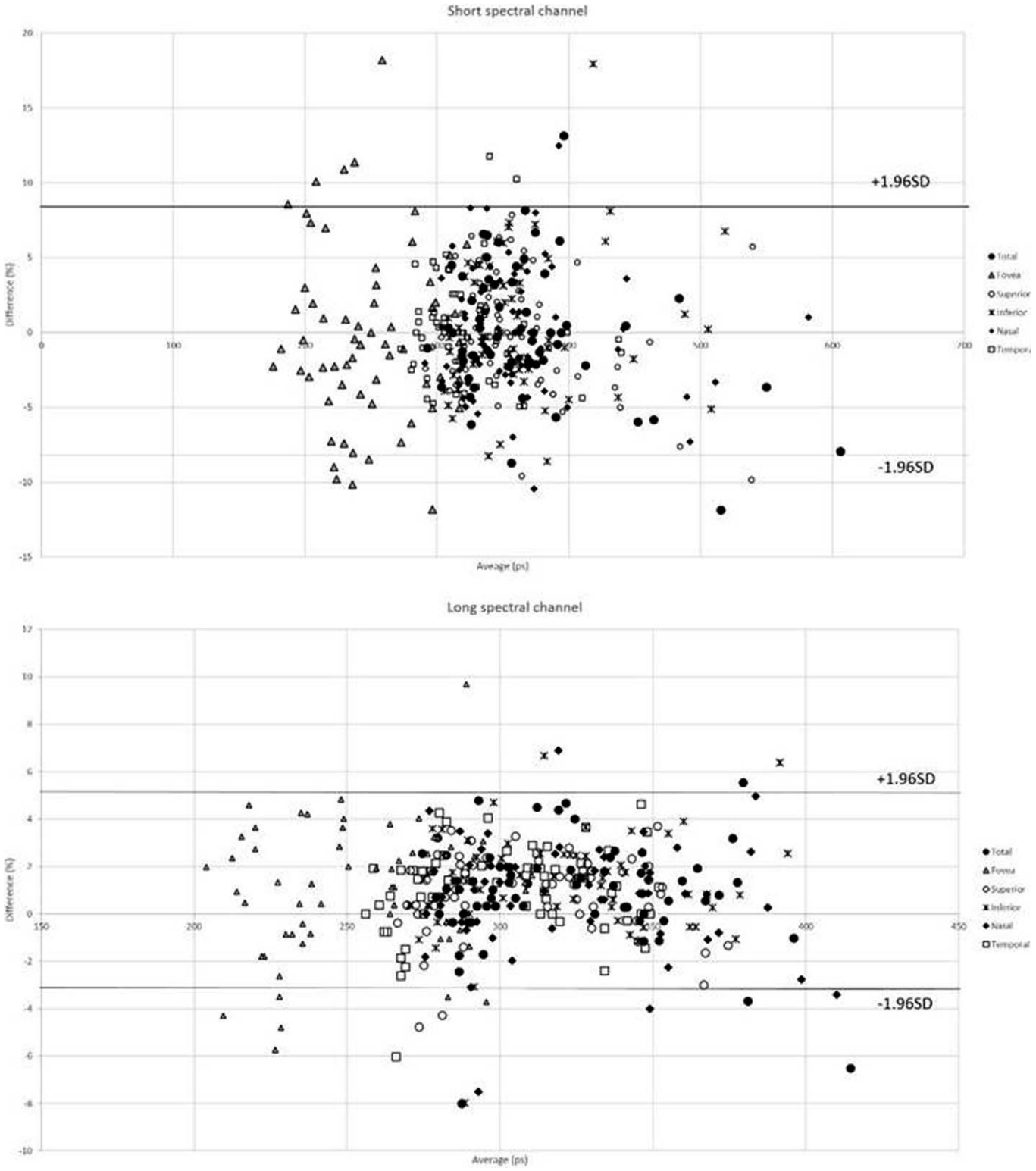

Figure 2. Combined Bland-Altman plot for repeatability of the first and second measurements in the SSC (short spectral channel) and LSC (long spectral channel).

Table 3. The Average and CV of Mean Fluorescence Lifetime (τ_m) of Each Retinal Area

	SSC		LSC	
Area	Mean ± SD, ps	CV, %	Mean ± SD, ps	CV, %
Total	367.8 ± 58.1	16	322.5 ± 34.00	11
Fovea	248.9 ± 40.8	16	255.4 ± 28.9	11
Superior	362.4 ± 50.7	14	310.8 ± 29.2	9
Inferior	363.0 ± 50.6	14	318.9 ± 32.7	10
Nasal	360.4 ± 54.0	15	323.5 ± 34.8	11
Temporal	324.1 ± 35.3	11	301.0 ± 28.5	9

(16% and 11% in SSC and LSC, respectively) than the other macular regions in both spectral channels (9%∼15%; Table 3)

Analysis of Individual Fluorescence Lifetime Components

Since τ_m is the amplitude weighted mean fluorescence lifetime, which consists of multiple fluorescence lifetime components, individual lifetime components were analyzed further to determine the component that accounted for the differences in the temporal area. Pseudocolor images of each fluorescence lifetime (τ_{1-3}) and amplitude from the short spectral channel (α_{1-3}) were generated to evaluate each component (Fig. 4). The fluorescence lifetime was shorter in the foveal region, but was relatively similar among the other four regions (Figs. 4B–D). The amplitude, however, was higher temporally (Fig 4F–H). Distribution histograms of all pixels were generated for each decay component (τ_{1-3}), by plotting the lifetime (x-axis) against the corresponding amplitude ($\alpha_{1-3;}$ y-axis) to track each pixel in the superior and temporal defined regions (Fig. 5). The fluorescence lifetime distribution of the superior macular region was shifted toward higher intensities and shorter lifetimes compared to the temporal retinal region (Fig. 5 C, D).

Correlation of Fluorescence Lifetime with Other Factors

Age and Refractive Error

The τ_m showed a positive correlation with age in all defined areas for both channels (Table 4, Fig. 6).

With regards to refractive error, there was no correlation of fluorescence lifetime with spherical equivalent in both spectral channels (Pearson correlation, $P > 0.05$).

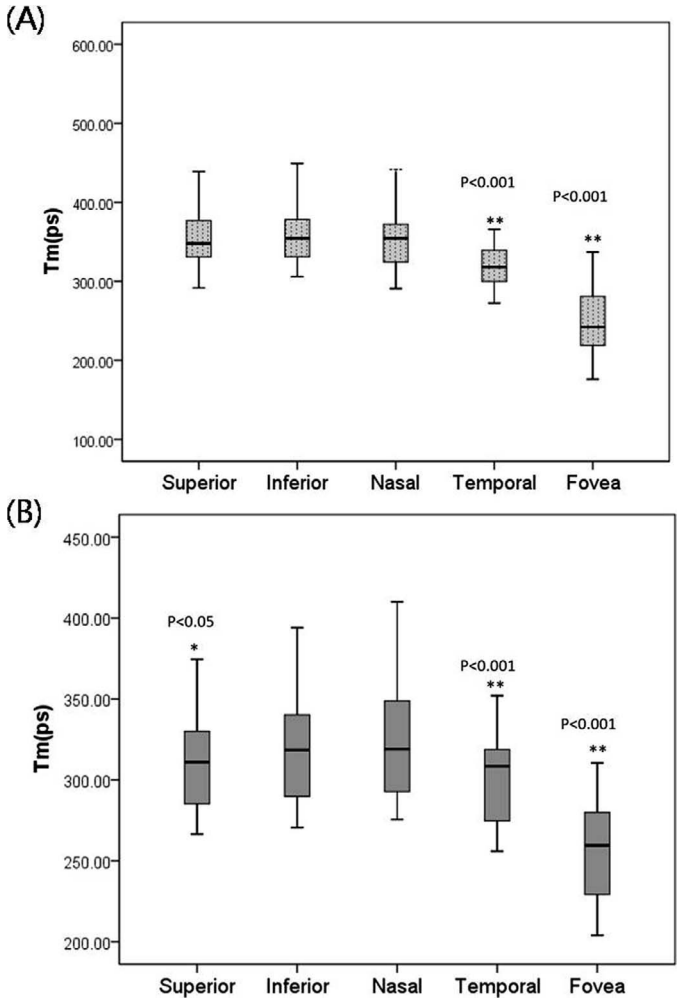

Figure 3. Differences in mean fluorescence lifetime of each retinal region in the SSC (channel 1, A) and LSC (channel 2, B). *Box*: median and 25%/75%; *whiskers*: 10%/90%. Student *t*-test *$P < 0.05$, **$P < 0.0001$).

Retinal Thickness and Vascular Density

We evaluated the correlation between τ_m and retinal thickness in the five predefined macular regions. Since the shortest τ_m values are found in the foveal region, which is thought to be due to the influence of macular pigment on the lifetime,[14] the correlation analyses were performed using the non-foveal regions. There was significant correlation of the retinal thickness with τ_m in both channels ($R = 0.298$, $P < 0.001$ in SSC and $R = 0.322$, $P < 0.001$ in LSC, Table 5, Fig. 7).

The VD of the whole macular region was 33.0% ±

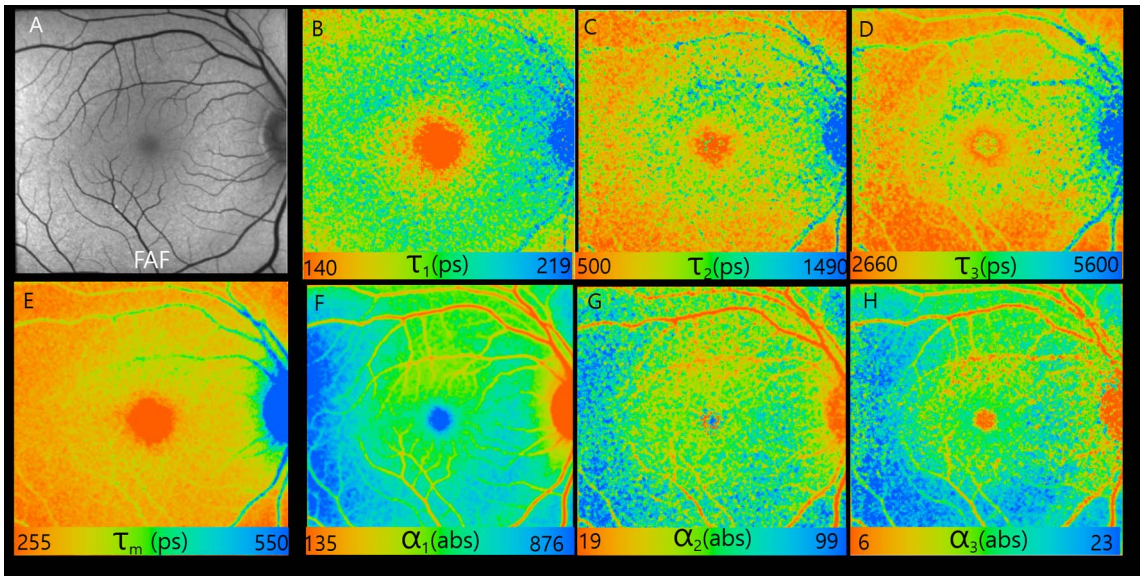

Figure 4. Autofluorescence image (A) of a normal eye with pseudocolor images (B–H) of the various FLIO parameters (mean lifetime and the various components used to compute the mean lifetime), contributing to the mean lifetime. Pseudocolor images of (B) τ_1, (C) τ_2, (D) τ_3, (E) τ_m, (F) a_1, (G) a_2, and (H) a_3.

3.0%, and for the subregions the VDs were 33.0% ± 3.8%, 33.9% ± 6.5%, 32.5% ± 7.4%, 36.9% ± 2.5%, and 36.0% ± 3.2% for the fovea, superior, inferior, nasal, and temporal macula, respectively. There was no significant difference in vascular density among the regions of interest (ROIs; Fig. 8B). There was a weak negative correlation between vascular density and the τ_m for the LSC ($R = -0.119$, $P = 0.040$), but

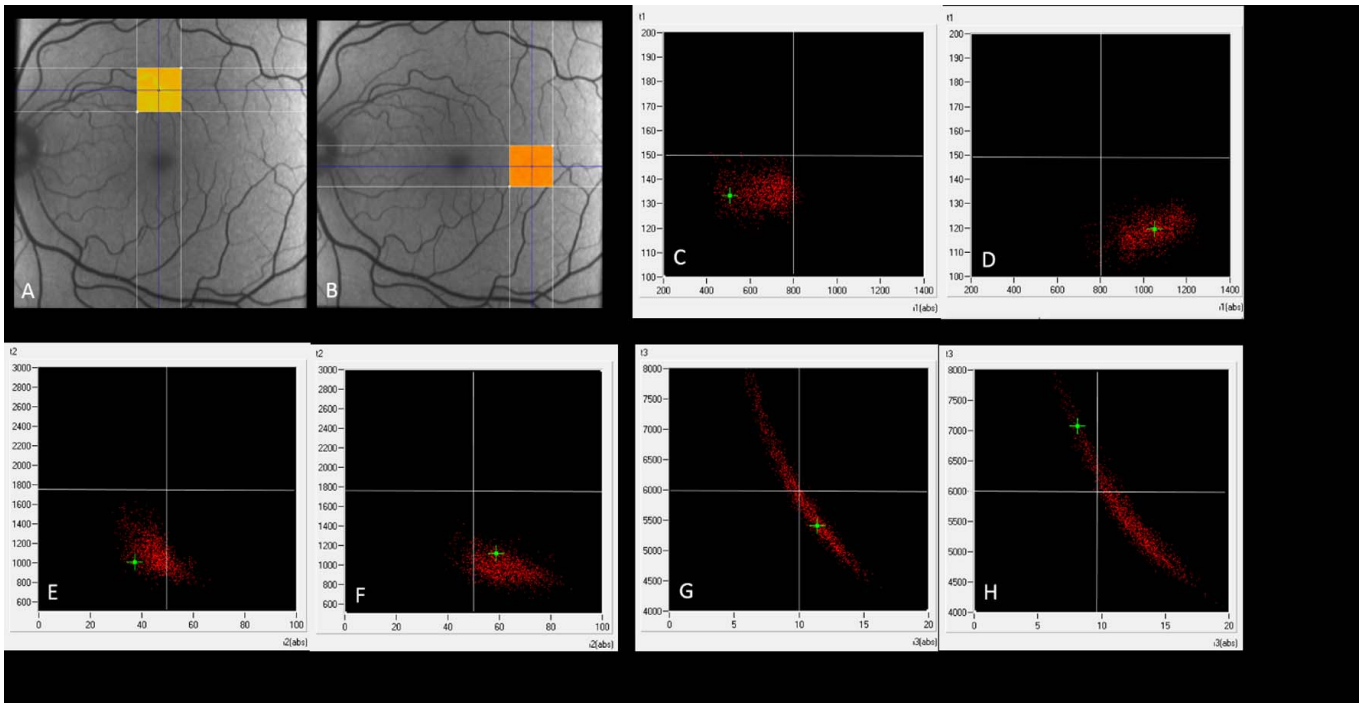

Figure 5. Distribution of lifetime (*y*- versus corresponding amplitude for all pixels in the superior and temporal macular regions. (A, B) Predefined retinal regions in the superior and temporal macula of the autofluorescence image. Distribution histograms with lifetime (C, D) t1 versus amplitude a1, (E, F) τ_2 versus amplitude a_2, and (G, H) τ_3 versus amplitude a_3 for the superior and temporal regions.

Table 4. The Correlation Fluorescence Lifetime with Age

	Total		Fovea		Superior		Inferior		Nasal		Temporal	
	r	*P*	*r*	*P*	*r*	*P*	*r*	*P*	*r*	*P*	*r*	*P*
SSC	0.588	0.000	0.686	0.000	0.494	0.000	0.505	0.000	0.607	0.000	0.571	0.000
LSC	0.584	0.000	0.667	0.000	0.477	0.000	0.508	0.000	0.605	0.000	0.548	0.000

$P < 0.05$.

this was not statistically significant for the SSC ($R = -0.112$, $P = 0.055$; Table 5, Fig. 8).

Discussion

Dysli et al.[5] reported good repeatability of fluorescence lifetime using FLIO in healthy subjects. However, evaluation of repeatability with a nondilated pupil could be a potential limitation because of stronger fluorescence lifetime effects of the crystalline lens. Also, they used a standardized Early Treatment of Diabeti Retinopathy Study (ETDRS) grid for topographic distribution of lifetimes within the macula. In this manner, lifetime distribution of fovea, and the inner and outer rings could be analyzed, but the lifetime differences among superior, inferior, nasal, and temporal cannot be explored easily. We found good repeatability of fluorescence lifetime following mydriasis in the whole retina, and five different retinal zones in healthy subjects. Generally, for assessing reproducibility, analysis of exactly the same field of view is essential, because a small shift in the image position can yield large differences in the lifetime. Despite this anticipated problem, the repeatability of τ_m for the entire macula actually was as good as the individual ROIs in our study.

We previously reported the impact of mydriasis on FLIO measurement.[10] We observed that FLIO without mydriasis results in a longer τ_m in the SSC and also takes a longer time for image acquisition. In addition to implementing pupil dilation, we also applied a different strategy for evaluating FLIO data. Since the fluorescence lifetimes are measured throughout the entire retinal depth, the observed signals can be derived from a variety of different fluorophores. Typically, multiple fluorophores are excited simultaneously and the measured fluorescence decay represents the superposition of all individual decay components, which must be fitted into a multiexponential decay model, which is a well-established statistical exercise.[15] Therefore, to calculate fluorescence lifetimes from every single pixel, the exponential decay curves are representing the most prominent fluorophores. Generally, previous FLIO reports have applied a biexponential or triexponential curve fit to the FLIO data, and previous studies evaluated the repeatability of FLIO in healthy subjects applying biexponential decay curves.[5–9] Dysli et al.[15] reported that a biexponential curve fit appeared to be a useful strategy for evaluating FLIO data for most diseases. In our study, triexponential decay curve was applied for evaluating FLIO data. The use of higher order exponents can facilitate discrimination of more fluorophores, but higher exponents also require more photons for analysis, which may affect the repeatability of the study. In a pilot study in our center (unpublished) we observed a higher number of erroneous pixels, which the instrument displays as blue dots with a higher χ^2 value, in lifetime images derived from a biexponential fitting curve compared to a triexponential fitting curve. Given these differences between the two fitting strategies we deemed that the repeatability needed to be evaluated using the triexponential fitting strategy. To our knowledge, the repeatability of FLIO following mydriasis using a triexponential fit has not been evaluated. This is essential to establish, particularly in a normal population, before mydriatic FLIO imaging and triexponential fitting can be used evaluate eyes with disease.

Table 5. The Correlation of Retinal Thickness and Vascular Density With Fluorescence Lifetime

	Retinal Thickness		Vascular Density	
	r	*P*	*r*	*P*
SSC	0.298	0.000	−0.112	0.055
LSC	0.322	0.000	−0.119	0.040

$P < 0.05$.

Mean fluorescence lifetime ranged from 124 to 390 ps for SSC, and 189 to 355 ps in the LSC. Interindividual CVs in the fovea were 17% for the SSC and 11% for the LSC, and 6% to 12% for the inner and outer ETDRS ring areas in a previous study.[5] Moreover, mean fluorescence lifetime in the

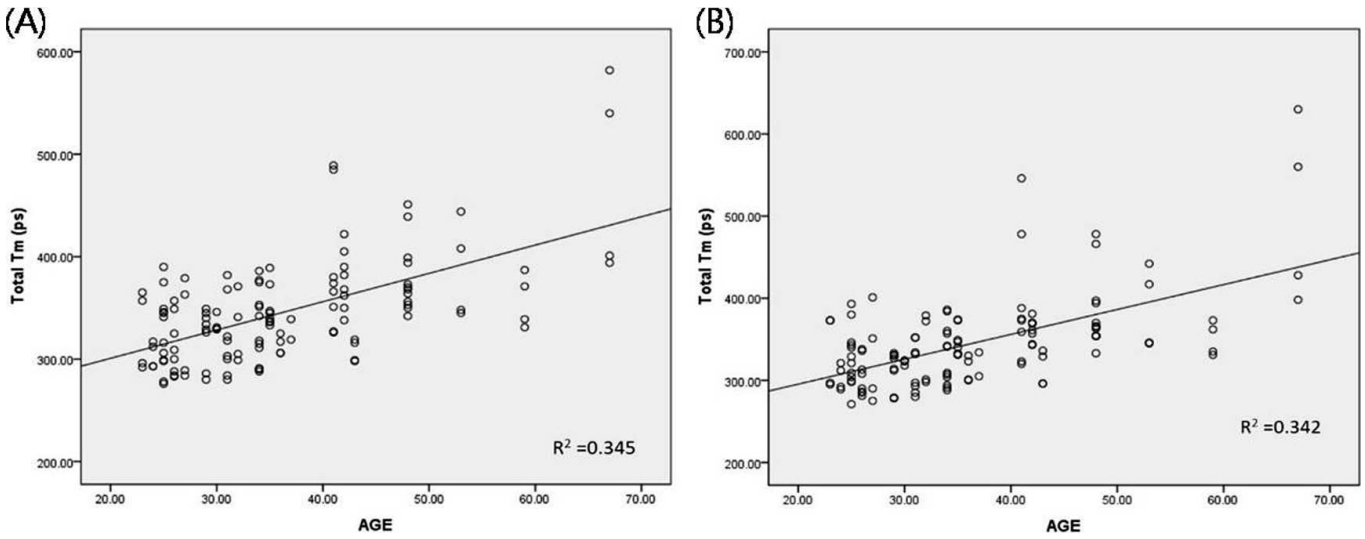

Figure 6. Correlation of mean fluorescence lifetime with age in both channels. (A) SSC. (B) LSC (Pearson's correlation, $P < 0.05$).

SSC was considerably shorter than that in the LSC. In our study, mean fluorescence lifetime ranged from 240 to 370 ps for SSC, and from 250 to 320 ps for LSC. Similar to previous studies, our interindividual CVs were 16% and 11% in the foveal region and 9% to 16% in other areas for the SSC and LLC, respectively. We presumed that the differences in absolute lifetime values between our study and previous reports reflects the different exponential decay curve analysis strategies, which highlights the importance of maintaining a consistent method across a study.

It is well known that the shortest τ_m are found in the foveal region, but the finding that τ_m in the temporal area for both channels, and τ_m of the nasal area in the SSC, are shorter than other areas has not been reported previously to our knowledge.[5–9] Similar to our study, Klemm et al.[10] reported the distribution of fluorescence often was inhomogeneous and fluorescence lifetime generally was independent of intensity. Greenberg et al.[16] also reported that autofluorescence intensities were greatest superotemporally and considered nonuniformities as instrument noise or the result of slight misalignment. In our study, we noted increased autofluorescence intensities in the temporal area during analysis of individual lifetime components, and also observed shorter lifetimes for

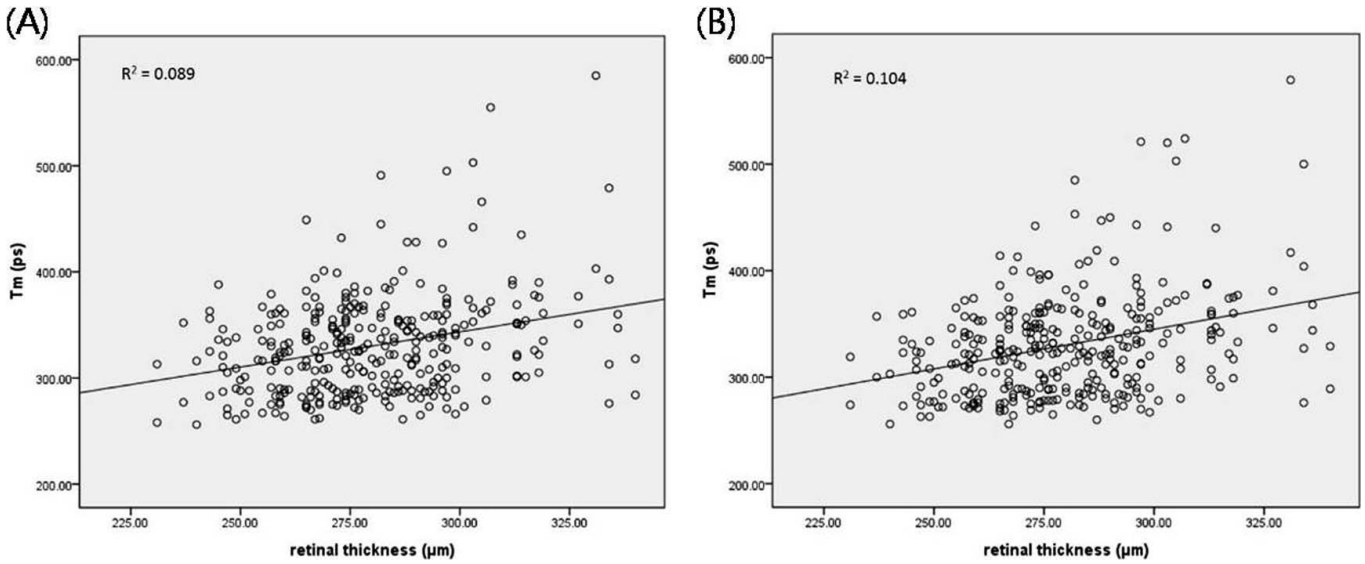

Figure 7. Correlation of mean fluorescence lifetime with retinal thickness. (A) SSC. (B) LSC (Pearson's correlation, $P < 0.05$).

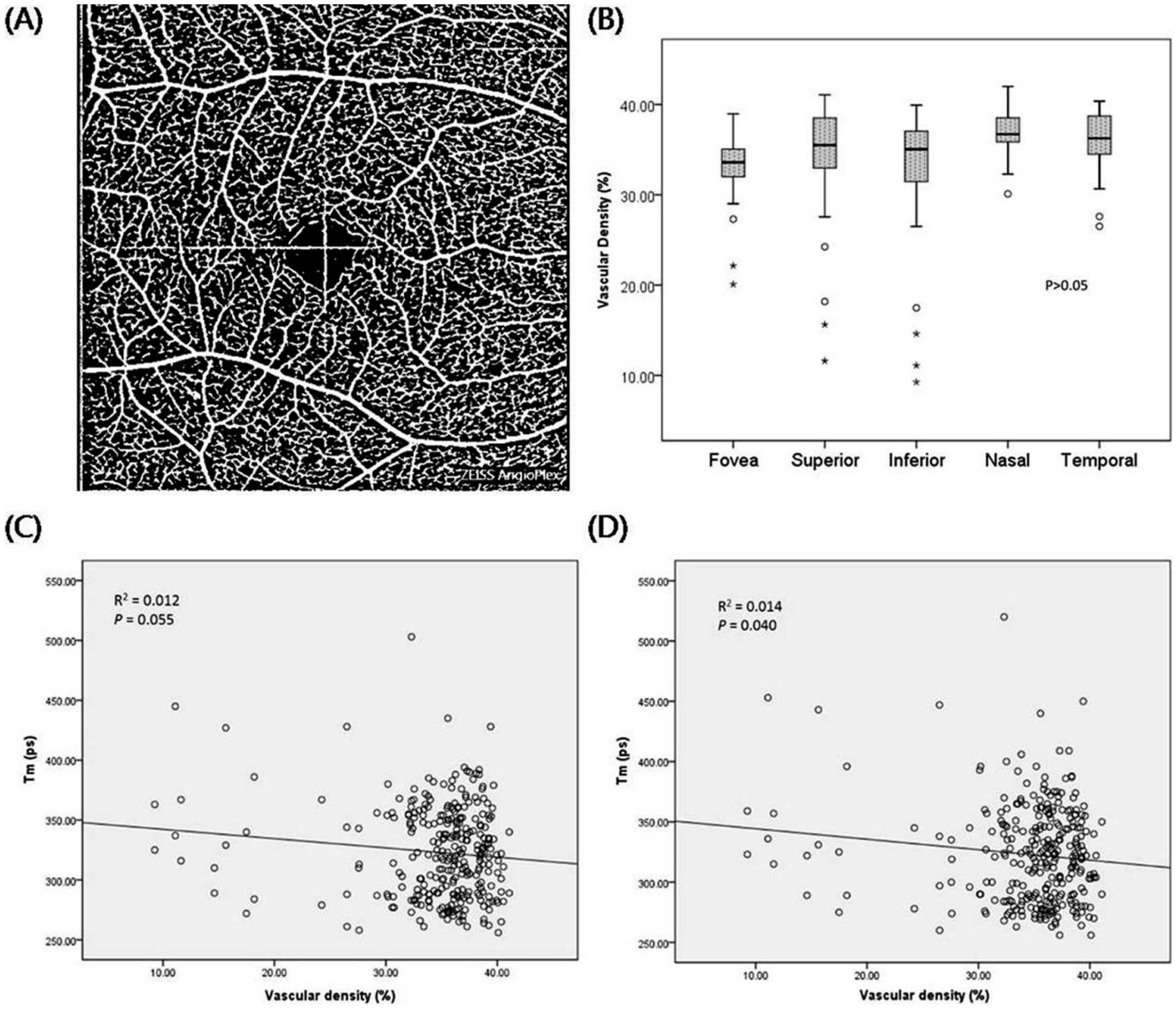

Figure 8. Correlation of mean fluorescence lifetime with retinal vascular density. (A) Final binarized image for calculating vascular density. (B) Vascular density in different retinal regions. (*Box*: median and 25%/75%; *whiskers*: 10%/90%). (C, D) Correlation of mean fluorescence lifetime with vascular density in (C) the SSC (Pearson's correlation, $R^2 = 0.012$, $P = 0.055$) and (D) the LSC (Pearson's correlation, $R^2 = 0.014$, $P = 0.040$).

the components (Figs. 4, 5). The explanation for the difference in the temporal macula is uncertain, and warrants further investigation. Although subtle misalignment (e.g., decentration of the imaging from the exact center of the pupil) could be a contributor, we do not believe this fully explains our findings. We speculated that differences in vascular density could be contributing factors. The vascular density in our study was slightly higher (though not statistically significant) in the temporal and nasal regions, and showed a negative correlation with fluorescence lifetime. It is well known that vessels always show longer lifetime in FLIO images, a finding that has been attributed to the high collagen content in vessels.[5] However, most vessels in these regions were capillaries (not arterioles), and capillary walls are very thin and lack collagen. In addition, vessel density would not explain why the nasal retina did not also show a shorter τ_m in LSC.

Similar to previous reports, we observed that τ_m increased with age and retinal thickness.[5–8] Greenberg et al.[16] speculated that this might be due to lipofuscin

accumulation with increasing age. A large volume and the strong autofluorescence of the crystalline lens could be another reason for age dependency of τ_m. Interestingly, our study results indicated that the correlation of age with τ_m in the SSC was stronger than with the LSC (Fig. 6). Schweitzer et al.[6] reported that the crystalline lens had more of an effect on τ_3 of SSC than τ_3 of LSC. We hypothesized that, because we used the triexponential curve, which included τ_3 for τ_m calculation, τ_3 was more influenced by the crystalline lens in SSC, which resulted in higher correlation of τ_m with age in the SSC in our study.

In conclusion, FLIO techniques using a triexponential decay function yield fairly repeatable fluorescence lifetime values in healthy phakic participants following dilation. Mean fluorescence lifetimes in the fovea and temporal macula showed a shorter lifetime compared to other regions in the macula. In addition to age, retinal thickness and retinal vascular density also appeared to have some impact on lifetime values. These various factors that impact lifetime values should be considered when evaluating FLIO results in the setting of disease.

Acknowledgments

The authors thank Ali Tafreshi, BS, Yoshihiko Katayama, PhD, from Heidelberg Engineering GmBH, Heidelberg, Germany, for providing technical assistance for the FLIO

Disclosure: **S. Kwon**, None; **E. Borrelli**, None; **W. Fan**, None; **A. Ebraheem**, None; **K.M. Marion**, None; **S.R. Sadda**, Optos, Carl Zeiss Meditec, Centervue (F,C), Heidelberg Engineering, Topcon Medical Systems, Nidek (F)

References

1. Schweitzer D, Schenke S, Hammer M, et al. Towards metabolic mapping of the human retina. *Microsc Res Tech*. 2007;70:410–419.
2. Delori FC, Dorey KC, Staurenghi G, et al. In vivo fluorescence of the ocular fundus exhibits retinal pigment epithelium lipofusin characteristics. *Invest Ophthalmol Vis Sci*. 1995;36:718–729.
3. Ishibashi T, Murata T, Hanagai M, et al. Advanced glycation end products in age related macular degeneration. *Arch Ophthalmol*. 1998; 116:1629–1632.
4. Schweitzer D, Hammer M, Schwietzer F, et al. In vivo measurement of time-resolved autofluorescence at the human fundus. *J Biomed Opt*. 2004;9: 1214–1222.
5. Dysli C, Quellec G, Abegg M, et al. Quantitative analysis of fluorescence lifetime measurements of the macula using the fluorescence liftime imaging ophthalmoscope in healthy subjects. *Invest Ophthalmol Vis Sci*. 2014;55:2106–2113.
6. Schweitzer D, Deutsch L, Klemm M, et al. Fluorescence lifetime imaging ophthalmoscopy in type 2 diabetic patients who have no signs of diabetic retinopathy. *J Biomed Opt*. 2015;20:61106.
7. Dysli C, Wolf S. Zinkernagel MS. Autofluorescence lifetimes in geographic atrophy in patients with age-related macular degeneration. *Invest Ophthalmol Vis Sci*. 2016;57:832–841.
8. Jentsch S, Schweitzer D, Schmidtke KU et al. Retinal fluorescence lifetime imaging ophthalmoscopy measures depend on the severity of Alzheimer's disease. *Acta Ophthalmol*. 2015;93:e241–247.
9. Dysli C, Wolf S, Hatz K, Zinkernagel MS. Fluorescence lifetime imaging in Stargardt disease: potential marker for disease progression. *Invest Ophthalmol Vis Sci*. 2016;57:832–841.
10. Sadda SR, Borrelli E, Fan W, et al. Impact of mydriasis in fluorescence lifetime imaging ophthalmoscopy. PloS One. 2018;13:e0209194.
11. Klemm M, Dietzel A, Haueisen J, et al. Repeatability of autofluorescence lifetime imaging at the human fundus in healthy volunteers. *Curr Eye Res*. 2013;38:793–801.
12. Kim, AY, Chu Z, Shahidzadeh A, et al. Quantifying microvascular density and morphology in diabetic retinopathy using spectral-domain optical coherence tomography angiography. *Invest Ophthalmol Vis Sci*. 2016;57:362–370.
13. Uji, A, Balasubramanian S, Lei J, et al. Impact of multiple en face image averaging on quantitative assessment from optical coherence tomography angiography images. *Ophthalmology*. 2017;124: 944–952.
14. Sauer L, Schweitzer D, Ramm L, et al. Impact of macular pigment on fundus autofluorescence lifetimes. *Invest Ophthalmol Vis Sci*. 2015;56: 4668–4679.
15. Dysli C, Wolf S, Berezin MY, et al. Fluorescence lifetime imaging ophthalmoscopy. *Prog Retin Eye Res*. 2017;60:120–143.
16. Greenberg JP, Duncker T, Woods RL, et al. Quantitative fundus autofluorescence in healthy eyes. *Invest Ophthalmol Vis Sci*. 2013;54:5684–5693.